Cellulose (2014) 21:4405–4418
DOI 10.1007/s10570-014-0440-y

ORIGINAL PAPER

Characterization of chitosan microparticles reinforced cellulose biocomposite sponges regenerated from ionic liquid

Fangbing Lv · Chaoxia Wang · Ping Zhu · Chuanjie Zhang

Received: 15 April 2014 / Accepted: 9 September 2014 / Published online: 13 September 2014

Abstract The chitosan-microparticles reinforced cellulose biocomposite sponges regenerated from ionic liquid were prepared and characterized. Fourier transform infrared (FTIR) spectroscopy confirmed that the cellulose dissolved in 1-allyl-3-methylimidazolium chloride without derivatization. Chitosan particles as reinforcement were incorporated into the cellulose matrix. FTIR spectra indicated hydrogen bonding between hydroxyl groups of cellulose and chitosan. The biocomposite sponges showed uniform three-dimensional interconnected porous structures. The breaking strength of the sponges increased significantly, from 0.09 to 0.32 MPa with the addition of 1.0 wt% chitosan. The sponges also demonstrated excellent antibacterial activity against *S. aureus* and *E. coli* with the average inhibition zone diameters >2 mm and the inhibition rate higher than 80 %. Furthermore, the biocomposite sponges exhibited good moisture penetrability and high porosity. The water uptake ability of the sponge was >25 times of its weight in water with a fast swelling. The chitosan/cellulose composite sponge is expected to be a promising material for potential applications as wound dressing.

Keywords Cellulose · Chitosan · Biocomposite sponge · Reinforced · Antibacterial

F. Lv · C. Wang (✉)
Key Laboratory of Eco-Textile, Ministry of Education, Jiangnan University, Wuxi 214122, China
e-mail: wangchaoxia@sohu.com

F. Lv · P. Zhu · C. Zhang
Key Laboratory of Biomass Fibers and Eco-Dyeing and Finishing in Hubei Province, Wuhan Textile University, Wuhan 430073, China

P. Zhu (✉)
State Key Laboratory of New Fiber Materials and Modern Textiles, Qingdao University, Qingdao 266071, China
e-mail: pzhu99@163.com

Introduction

Cellulose is currently one of the most promising bio-based polymeric resources (Novotna et al. 2013). Because of the increasing demand for environmentally friendly and biocompatible products, numerous new functional materials from cellulose are being developed for biomedical applications (Chang and Zhang 2011). Biomaterial sponges are becoming increasingly important (Nair and Laurencin 2007) in biomedical applications such as wound dressing, drug delivery and tissue engineering. Moreover, cellulose having abundant hydroxyl groups can be easily prepared into hydrogels with fascinating structures and properties (Pei et al. 2013). The suitability of viscose cellulose sponges as scaffold for cartilage tissue engineering has been investigated, indicating that cellulose sponges are biocompatible for at least 4 weeks in cultivation (Pulkkinen et al. 2006). However, the lack of solubility

of cellulose in water and common organic solvents brings difficulties in its processability and functionality (Jin et al. 2007; Zhang et al. 2010).

As a new class of solvents, ionic liquid can be used for cellulose regeneration (Swatlosti et al. 2002; Feng and Chen 2008; Rogers and Seddon 2003). Ionic liquids have received much attention due to their attractive properties including good chemical and thermal stability, non-flammability and ease of recycling (Heinze et al. 2008). By changing the regeneration instrument and process, regenerated cellulose materials can be adopted in various forms, such as films, sponges, beads and fibers. Micro- and nanoporous materials have been prepared by processing cellulose with 1-allyl-3-methylimidazolium chloride ([AMIM]Cl) and supercritical CO_2 (Tsioptsias et al. 2008). Nanoporous cellulose foams can be obtained by dissolving cellulose in [BMIM]Cl and freeze drying the solution with liquid N_2 (Deng et al. 2009). Even though the cellulose porous materials have good sorption capacity and wettability rate, the antibacterial and mechanical properties are still not satisfactory (Wu et al. 2004). Controlling bacterial or fungal growth on cellulose porous materials can be achieved using biologically active polymers by the inclusion of antimicrobial components, e.g. collagen and chitosan.

Chitosan is a cationic biopolymer composed of glucosamine and N-acetyl-glucosamine, which is obtained by the partial de-acetylation of chitin (Mohamed and EI-Ghany 2012; Jayakumar et al. 2010; Muzzarelli 2009). Being biocompatible and biodegradable with haemostatic and antimicrobial properties, chitosan and chitosan-based composites are protagonists in wound healing (Jayakumar et al. 2011). For instance, chitosan–pectin–TiO_2 nano dressing materials for wound healing (Archana et al. 2013a), chitosan–PVP–TiO_2 wound dressing materials (Archana et al. 2013b) and chitosan–pectin–alginate scaffolds for tissue engineering (Archana et al. 2013c) have been prepared. These composite structures exhibited high swelling property, excellent antibacterial activity and cell-viability as well as good mechanical strength. Chitosan sponges have been studied for bone regeneration (Park et al. 2000; Lee et al. 2000; Lai et al. 2003) and as media for pancreatic islets culture (Cui et al. 2001), as well as for wound dressings in which antibiotics could be included (Mi et al. 2001, 2002). Chitosan sponges provide non-toxicity, favorable mechanical properties and capacity for bioresorption of the constituent materials (Kofuji et al. 2001; Singla and Chawla 2001).

To assimilate the beneficial properties of both cellulose and chitosan, a porous sponge from a composite of cellulose and chitosan was developed. The chitosan/cellulose composite beads, films, and membranes have been prepared using LiCl/*N*,*N*-dimethylacetamide system, NaOH/thiourea aqueous solution (Kondo et al. 2004; Morgado et al. 2011; Liang et al. 2007; Zhang et al. 2002) and ionic liquids ([BMIM]Ac, [AMIM]Br and [BMIM]Cl) (Stefanescu et al. 2012; Takegawa et al. 2010). Bio-based nanocomposite films have been successfully developed using cellulose whiskers as the reinforcing phase and chitosan as the matrix (Li et al. 2009).

Although considerable efforts have been devoted to the development of composites based on cellulose and chitosan as the biomass resources, little work has been done on the chitosan microparticle-reinforced cellulose composite sponges. In this study, the biocomposite sponges were prepared using chitosan microparticles as the reinforcement and cellulose as the matrix with [AMIM]Cl as solvent during composite fabrication. Chitosan was first ground by a planetary ball mill. The obtained chitosan particles were added to enhance the mechanical and antibacterial properties of the cellulose sponges. The morphological and structural properties of cellulose composite sponges were analyzed by SEM and Fourier transform infrared (FTIR), respectively. Effects of chitosan particles contents on the porosity, the swelling ratio (SR) and the moisture vapour transmission rate were also investigated. Furthermore, antibacterial properties of the chitosan/cellulose composite sponges were studied. This paper provides a novel combination process of regenerated cellulose and chitosan particles for potential biomedical applications.

Materials and methods

Materials

Cotton fabrics (190 g/m^2, DP 850, knitted, white) supplied by the Wuhan First Cotton Group Co., Ltd., were used in this study. The degree of deacetylation of the chitosan sample was 84.5 %, as was estimated by elemental analysis data and the molecular weight was approximately 1.1×10^6. An ionic liquid, [AMIM]Cl

was purchased from Shanghai Chengjie Chemical Co., Ltd., China and dried in vacuum oven at 80 °C for 48 h before use. Anhydrous sodium sulphate as foaming agent, ethanol, sodium chloride and calcium chloride were obtained from Shanghai Medical Group Chemical Reagent Co. Ltd., China. These chemicals were analytical grade and used as received.

Preparation of chitosan microparticles

Dried chitosan was crushed using a planetary ball mill which was a vertical batch type mill (ND8, Tianzun electronic Co. Ltd. Nanjing). Ground samples were obtained by conditions that set the filling degree of agate balls at 30 %, grinding time at 6 h and rotating at 300 rpm. The agate ball to powder weight ratio was 25:1.

Preparation of chitosan/cellulose composite sponges

Bleached cotton fabrics and [AMIM]Cl were dried in vacuum oven at 80 °C for 48 h to remove residual water. The presence of water can significantly impair cellulose solubility in ionic liquid by competing with the ionic liquid for hydrogen bonds to the cellulose. The dissolving process was controlled by the silicone oil bath at 110 °C for 30 min until the dried cotton totally melted into [AMIM]Cl in a three-necked flask with mechanical stirring. The chitosan powders were slowly added into the cellulose/[AMIM]Cl solution with vigorous stirring for an additional 1 h.

Anhydrous sodium sulphate (300 wt% to the cellulose/[AMIM]Cl suspension) was added to the cellulose/chitosan/[AMIM]Cl suspension at 110 °C. The suspension was stirred for 30 min. The obtained suspension was cast on a polytetrafluoroethylene plate. The plate was then soaked with deionized water, and the water was replaced at an interval of 4 h for 6 times. The chitosan/cellulose hydrogels were quickly transferred to a refrigerator at −18 °C for 12 h, followed by lyophilization in a freeze drier (LGJ-10D, Sihuan Scientific Instrument Co., Ltd., Beijing, China) for 24 h. The preparation procedures for chitosan/cellulose composite sponges with [AMIM]Cl were shown in Fig. 1. After the coagulation of chitosan/cellulose composite sponges, the residual [AMIM]Cl in coagulation bath was recovered by the distillation of the water/[AMIM]Cl mixture under reduced pressure both in rotary evaporator and distilling apparatus.

Characterization

Particle size analysis

The particle size analysis of chitosan powders was performed with a Nano-ZS90 (Malvern Co. Ltd. UK). The powders which had been diluted to 1,000 times with ethanol were laid in the sample room at 25 °C and analyzed with the DTS software.

Fourier transform infrared (FTIR) spectroscopy

To analyze the various functional groups present in the composite sponges, FTIR measurements were performed using a FTIR spectrometer (Equinox 55, Bruker, German). The samples were finely ground and mixed with potassium bromide and pelletized. The pellets were scanned in the range of 500–4,500 cm^{-1}.

Scanning electron microscopy (SEM)

The morphologies of cellulose sponges with and without chitosan particles were analyzed by scanning electron microscope (JSM-5600LV, JEOL, Tokyo, Japan). The freeze-dried samples were sputter coated with gold and photographed at an accelerating voltage of 15 kV at magnifications of 50–250.

Porosity

The porosity of the cellulose sponges was determined by the liquid displacement method. Dimensions of the sponges were measured using a vernier caliper and the volume (V) was calculated. Deionized water was used as the displacing liquid. A sample of measured weight (W_i) was immersed in a graduated cylinder containing a known volume of ethanol and soaked for 24 h to allow water to penetrate into the pores of the sponge. The final weight of the wet sponge was noted as W_f. The porosity can be calculated using the following equation.

$$\text{Porosity } \% = (W_f - W_i)/(\rho_{water} \times V)$$

ρ_{water} : Density of water

Moisture vapour transmission rate (MVTR)

MVTR of the chitosan/cellulose composite sponges was determined in accordance with the standard test

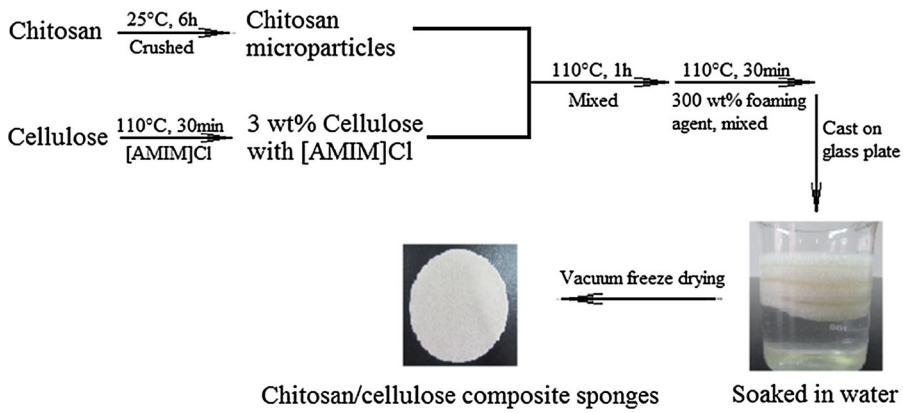

Fig. 1 Preparation procedures for chitosan/cellulose composite sponges with [AMIM]Cl

method, ASTM E96-90. The sponges were fixed securely over the container with the test fluid consisting of a solution of sodium/calcium chloride. The containers were weighed and placed in an incubator at 37 °C for a period of 48 h. The containers were reweighed periodically. The loss in weight due to passage of moisture vapour through the dressing was determined. The MVTR (g/m^2h) was calculated by the following equation:

$$\mathrm{MVTR} = (G/t)/A$$

where G is the weight loss of the samples (g), t is test time (h) and A is effective membrane area (m^2).

Swelling studies

Swelling studies of the chitosan/cellulose composite sponges were carried out by the following method. All sponges were equilibrated in a conditioning room with an atmosphere of 25 °C and 50 % relative humidity air for 48 h. The sample size was approximately 2 cm × 2 cm square with 1 cm in thickness.

Swelling kinetics of the sponges were measured in deionized water by determining the weight of the sponges at 37 °C at specific time intervals, after absorbing the excess liquid on the surface of the sponges by filter paper. The SR was calculated as follows:

$$\mathrm{SR}\ (g/g) = (W_t - W_0)/W_0$$

where W_t and W_0 are the weights of the swollen sample at time t and that of the original sample, respectively.

Mechanical test

The samples were cut into strip-shaped specimens with 10 mm in width and 30 mm between the grips. A universal testing machine (5560, Instron, USA) was used to determine tensile strength of the samples at an extension speed of 5 mm/min. The tensile strength was determined by averaging over five tests per sample.

Antibacterial activity evaluation

The antibacterial activities of the samples were estimated for the Gram-positive bacteria *S. aureus* (ATCC 6538) and the Gram-negative bacteria *E. coli* (ATCC 25922) according to the AATCC 100-2004 standard method. Inhibitory effects of the chitosan/cellulose composite sponges with different chitosan content were tested by the inhibition zone method and the shaking flask method, respectively. The reductions of bacteria were calculated according to the following equation:

$$R = (B - A)/B \times 100\ \%$$

where R is the reduction (%), A is the number of bacteria recovered from the inoculated treated test specimen swatches in the jar incubated over the desired contact period (24 h), B is the number of bacteria recovered from the inoculated treated test specimen swatches in the jar immediately after inoculation (at "0" contact time).

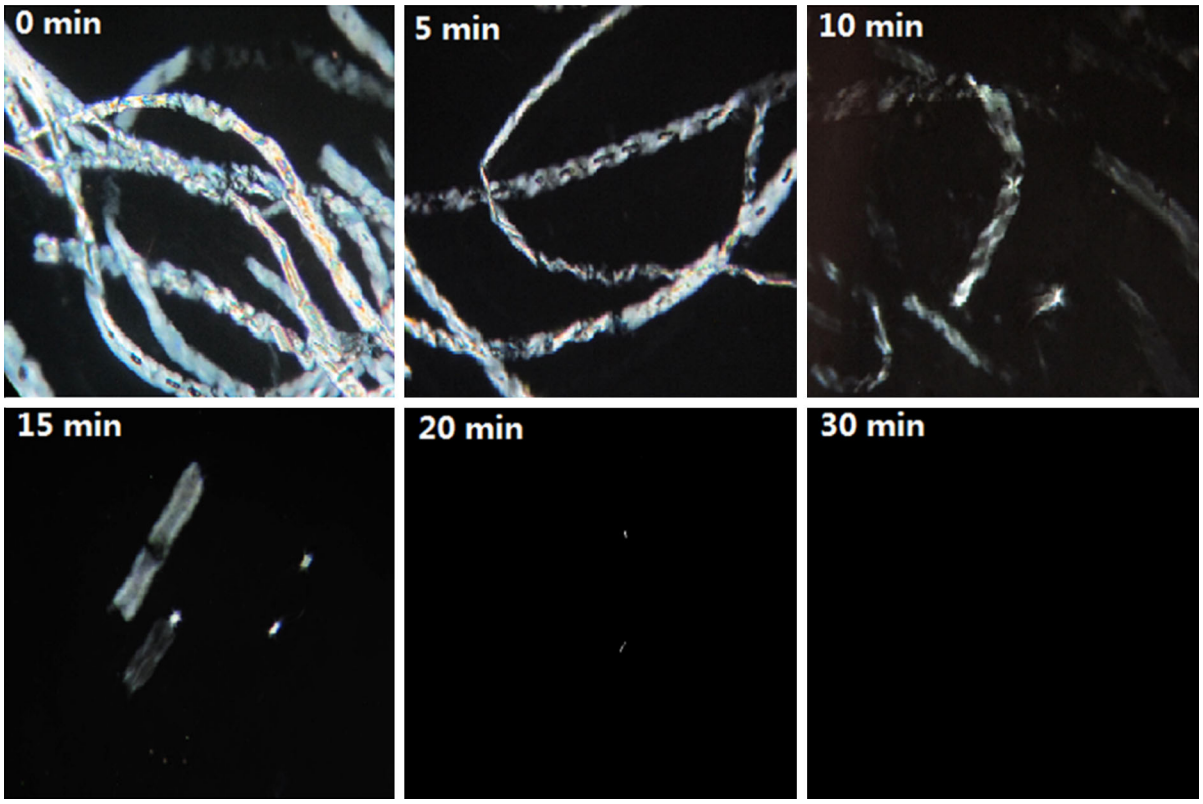

Fig. 2 Optical microscopic images of 3.0 wt% cotton fabrics dissolution in [AMIM]Cl at 110 °C

Results and discussion

Dissolution process of cotton fabrics in [AMIM]Cl

The dissolution process of cellulose in [AMIM]Cl was monitored by the disappearance of the highly crystalline cotton linter using a polarized light microscope, as shown in Fig. 2. Most of fibrous materials disappeared after only 10 min and the visual field became dark. Only a few bright spots could be observed after 15 min. A fully black field was obtained when the dissolution time was increased to 30 min. In general, the results consistently indicated that the cotton fabrics dissolved very quickly in [AMIM]Cl at 110 °C with a mechanism of fast dissolution by disintegration of the fibrous cellulose into fragments. Upon interaction of the cellulose-OH and [AMIM]Cl, the oxygen and hydrogen atoms from hydroxyl groups are separated, resulting in the breakage of the hydrogen bonds between the cellulose molecular chains, and then the cellulose dissolves (Cao et al. 2009).

Particle size analysis

The particle size distribution of chitosan powders was in a range of 0.8–1.5 μm as shown in Fig. 3. The average particle size as obtained from the number average weight distribution was approximately 1.2 μm with a PDI of 0.326. The narrow range of particle distribution indicated that the particle size distribution of chitosan powders was uniform. Finer particles tended to have a greater number of particles per unit weight. The finer particles were more likely to form a homogeneous cellulose/[AMIM]Cl solution, which was used for the preparation of the chitosan/cellulose composite sponges. The size of the chitosan particles played a crucial role in the performance of the composite sponges. It determined the distribution of chitosan particles in the composite sponges and the formation of porous structures, which could further influence the mechanical properties of the sponges.

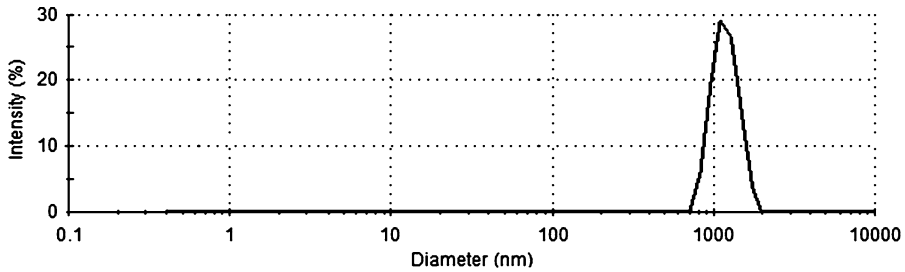

Fig. 3 Particle size distribution of chitosan powders

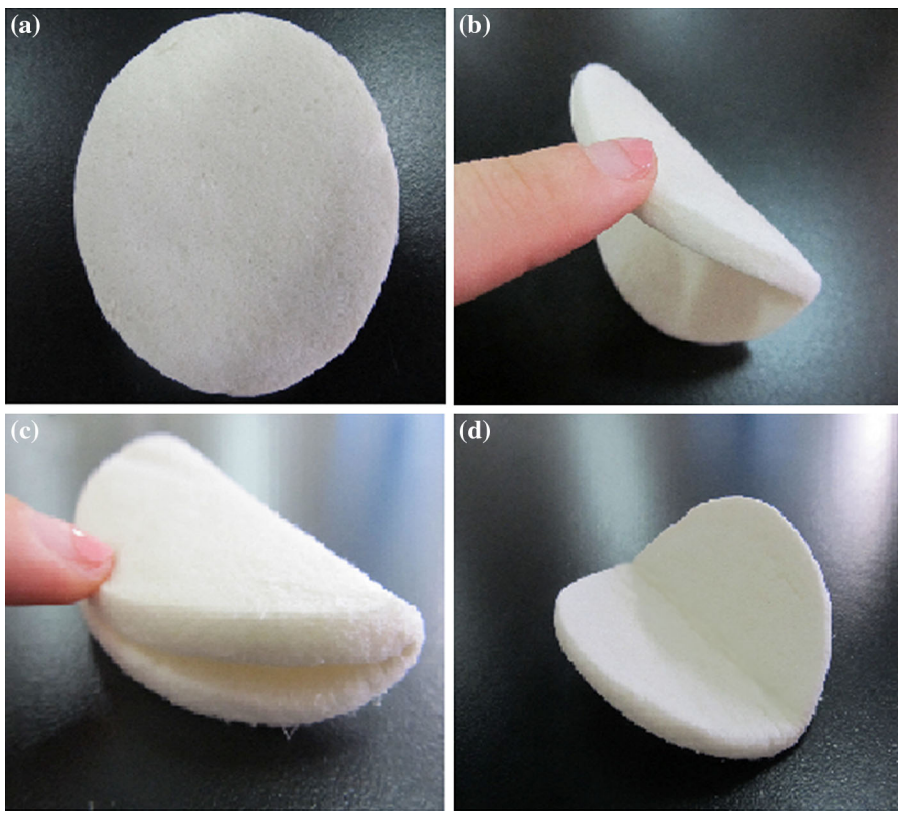

Fig. 4 Morphological images of the chitosan/cellulose composite sponges: (**a**) flattened sponge, (**b**) crooked sponge, (**c**) folded sponge and (**d**) recovered sponge

Morphology of chitosan/cellulose composite sponges

A flexible dry chitosan/cellulose composite sponge prepared via freeze drying is shown in Fig. 4. It can be observed that the surfaces of the composite sponges were relatively neat. Compact porous structures were uniformly distributed on the surface of the chitosan/cellulose composite sponge, indicating a good dispersion level of chitosan powders for the composite sponges. It was difficult to directly observe the single chitosan particle dispersion in the cellulose matrix due to its small particle size, which was supported by the results from the distribution of chitosan microparticles.

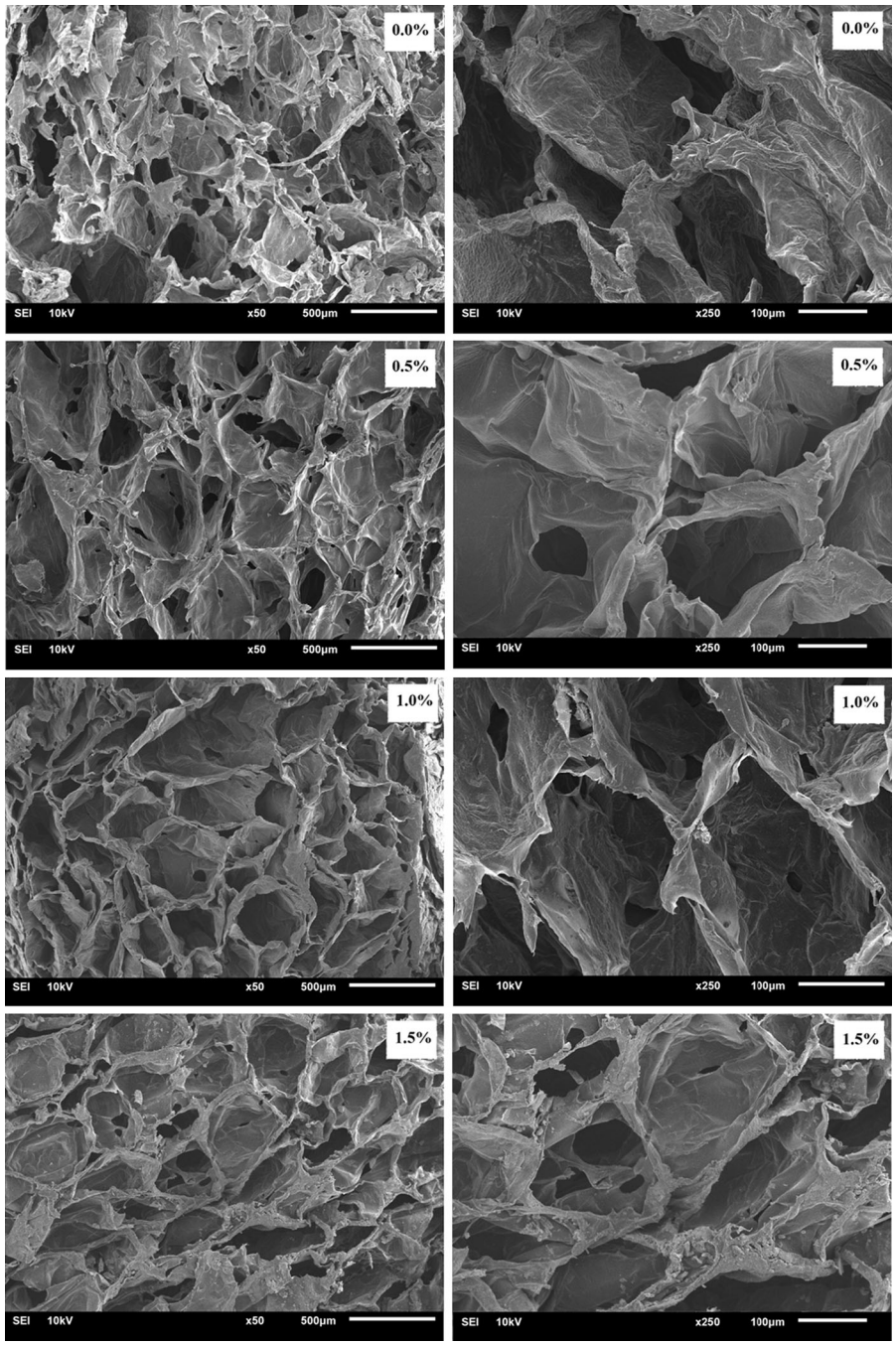

Fig. 5 SEM micrographs of the fracture surface of the cellulose composite porous sponges with different chitosan content (3.0 wt% cellulose)

The chitosan/cellulose composite sponge was very soft and could be deformed over a large range of strain. When the load was removed, the original shape was recovered indicating the good elasticity of the porous material at room temperature. Consequently, the chitosan/cellulose composite sponge exhibited excellent appearance and flexibility.

SEM micrographs of the prepared single cellulose and chitosan/cellulose composite sponges are shown in Fig. 5. As can be readily seen at a small

magnification, the cross section possessed a hierarchical structure with pores of different sizes. A higher magnification clearly illustrated that all the cellulose composite sponges showed three-dimensional interconnected porous structures. This could be attributed to the vacancies generated after the removal of water by freeze drying from the regenerated cellulose. After dissolution in [AMIM]Cl and subsequent coagulation with water, the regenerated swollen cellulose hydrogels were formed. During freeze drying the three-dimensional porous network structure of the cellulose hydrogels could be preserved with ice crystals acting as templates for the pore formation of the cellulose sponges.

Moreover, the porous structure for 1.0/3.0 wt% chitosan/cellulose composite sponge seemed to be better organized than that in the case of 3.0 wt% cellulose or 0.5/3.0 wt% chitosan/cellulose composite. With the incorporation of chitosan particles the cellulose composite sponges exhibited a highly porous structure with uniform distribution of pores. It was probably due to the strong intermolecular hydrogen bonds between cellulose and chitosan in the composite sponges. Additionally the chitosan particles acted as a reinforcing structure that partially prevented the collapse of the cellulose network, as supported by the results from mechanical tests (to be presented later). However, when the chitosan content was increased to 1.5 wt%, many chitosan particles were observed on the edge of the pores. The aggregation of chitosan particles would impede the formation of the pores.

FTIR analysis

As shown in Fig. 6, the FTIR spectrum of the regenerated cellulose sponge was similar to that of the original cotton fabric, indicating that no other chemical reaction occurred besides the breakage of hydrogen bonds during the processes of dissolution and regeneration. Cellulose dissolved in [AMIM]Cl directly, producing a cellulose solution without derivatization. Several characteristic bands of cellulose were located at 3,340 cm^{-1} corresponding to –OH stretching, 2,890 cm^{-1} corresponding to aliphatic C–H stretching, 1,470 cm^{-1} corresponding to $–CH_2$ bend, 1,040 cm^{-1} corresponding to asymmetric C–O–C stretching band and very strong signal at 930 cm^{-1} corresponding to symmetrical stretching band. The sharp peak at 860 cm^{-1} corresponded to the glycosidic C–H deformation with ring vibration contribution and O–H bending, which was characteristic of β-glycosidic linkages between glucose in cellulose, and it was observed only in the regenerated cellulose sponge (Jin et al. 2009). This might indicate that the crystal structure of cotton fabric was transformed from cellulose I to cellulose II (Raymond et al. 1995).

For the pure chitosan, the broad band at 3,300–3,500 cm^{-1} was assigned to the –NH– and –OH stretching vibrations. The chitosan spectra also showed two peaks at 1,657 and 1,595 cm^{-1}, which were attributed to amides I and amides II, respectively. For the chitosan/cellulose composite sponge, the absorption peak of the carbonyl band shifted to a lower frequency (1,640 cm^{-1}) suggesting that these carbonyl groups were involved in hydrogen bonding with the cellulose functional groups. The –NH bending in amides and amines was no longer observed in the spectra of the composite sponges because the band shifted to a higher frequency overlapping with the carbonyl stretch in amides. This shifting indicated that the –NH groups of chitosan were involved in hydrogen bonding with the functional groups of cellulose (Luo et al. 2008). The interaction between cellulose and chitosan was also identified by the hydroxyl group band present in the range of 3,300–3,500 cm^{-1}. The hydroxyl group band for the chitosan/cellulose composite sponge shifted from 3,340 cm^{-1} (the cellulose sponge without chitosan) to 3,400 cm^{-1}. The shift could be attributed to intermolecular interactions between the hydroxyl groups of cellulose and chitosan, which might disrupt hydrogen bonding between the cellulose molecules. This supported the notion that cellulose molecules and chitosan molecules were cross-linked by intermolecular forces to a certain extent. Moreover, the characteristic bands of [AMIM]Cl were located at 3,065 cm^{-1} corresponding to C–H stretching of imidazole rings and C–H asymmetrical stretching of $–CH_3$ on substituent groups, the characteristic absorption peak at 1,570 cm^{-1} corresponding to C=N stretching vibration of cationic imidazole rings, 668 cm^{-1} corresponding to C=C stretching vibration on allyl groups, 765 cm^{-1} corresponding to imidazole ring bending vibration. No characteristic absorption peak of [AMIM]Cl was observed in the spectrum of chitosan/cellulose composite sponges, indicating that there

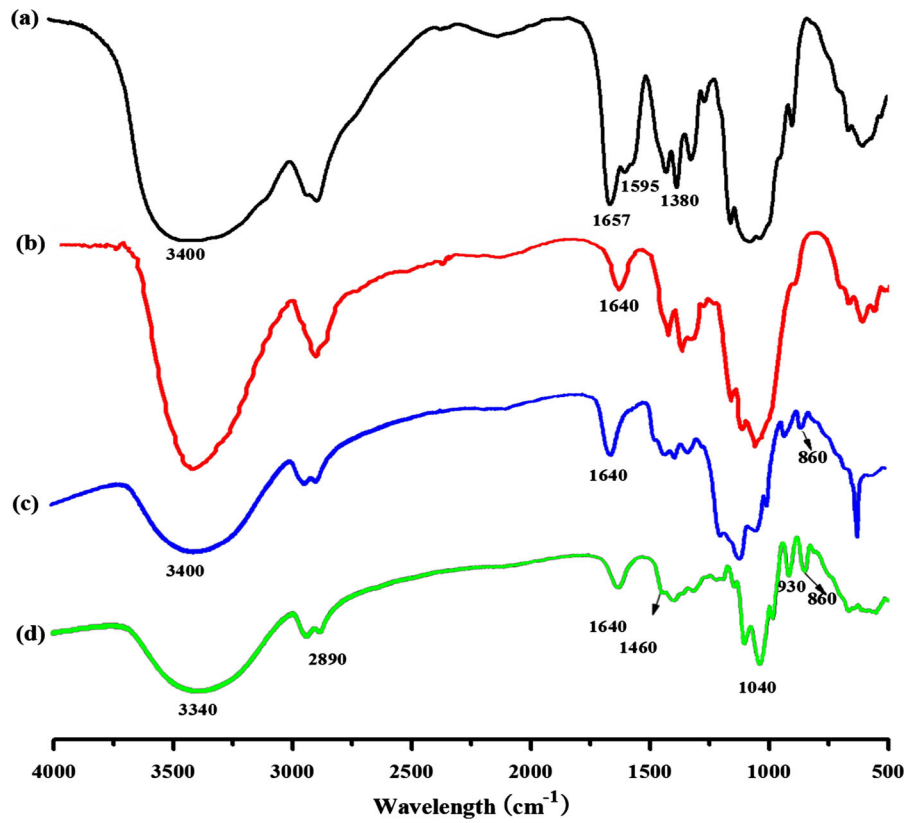

Fig. 6 FTIR spectra of different samples: (**a**) chitosan, (**b**) original cellulose, (**c**) regenerated chitosan/cellulose and (**d**) regenerated cellulose

was no residual solvent in the cellulose composite sponges.

Porosity and moisture vapour transmission rate (MVTR)

As shown in Table 1, the porosity of the cellulose sponge without chitosan particles was 60.1 %. The 3.0 wt% cotton fabric could dissolve in [AMIM]Cl effectively. Nevertheless, anhydrous sodium sulphate as the foam agent could not dissolve in [AMIM]Cl. When the cellulose was regenerated from cellulose/[AMIM]Cl solution in the coagulated bath, the dissolution of the foam agent resulted in a porous structure of the cellulose sponge. With an increase of chitosan content, the porosity of cellulose composite sponges increased from 60.1 to 75.9 %. The addition of chitosan particles into the cellulose generated hydrogen bonds with hydroxyl groups in cellulose molecules and improved the stability of the porous structure therefore increased the porosity.

Table 1 Porosity and MVTR of the chitosan/cellulose composite sponges with 3.0 wt% cellulose

Chitosan content (wt%)	Porosity (%)	MVTR at 24 h (g/m^{2}h)	MVTR at 48 h (g/m^{2}h)
0.0	60.1 ± 0.6	71.2 ± 0.7	64.8 ± 1.9
0.5	65.4 ± 1.5	83.7 ± 2.1	74.3 ± 2.0
1.0	72.7 ± 1.0	87.8 ± 1.5	77.6 ± 2.5
1.5	75.2 ± 1.3	89.1 ± 2.8	78.1 ± 1.2
2.0	75.9 ± 0.4	90.2 ± 0.8	78.9 ± 2.7

The moisture vapour transmission rate (MVTR) is a distinct factor that shows the potential of sponges as medical dressing in transmission of body liquids or wound exudates. The MVTR of cellulose sponges with different chitosan contents is presented in Table 1. The typical MVTR of normal skin is 8.5 g/(m^{2}h). The MVTR of injured skin varies in a broad range, from 11.6 g/(m^{2}h) for a first-degree burn to 214 g/(m^{2}h) for a granulating wound (Wu et al. 2004). The MVTR of the cellulose sponge without chitosan at

24 h was 71.2 g/(m^2h). Relatively higher MVTR was observed for the cellulose composite sponges with chitosan particles. The MVTR generally increased with increasing chitosan content. The MVTR of the chitosan/cellulose composite sponge with 2.0 wt% chitosan content at 24 h increased to 90.2 g/(m^2h), which demonstrated that the cellulose composite sponges could maintain a suitable moisture environment for low- and mid-range exudative wounds without excessive dehydration. However, the MVTR for all the cellulose composite sponges were found to decrease with time. This may have been caused by moisture absorbed into the pores which impeded vapour transmission.

The chitosan particles formed hydrogen bonding with hydroxyl groups in cellulose molecules and facilitated the formation of the porous structure. The presence of chitosan particles in the composite sponges would increase the MVTR due to stronger affinity of chitosan to water molecules, and due to the larger volume of $–NH_2$ side groups (19 cm^3/mol) on chitosan than that of the –OH side groups (13 cm^3/mol) on cellulose (Shieh and Huang 1998). As a consequence, the chitosan/cellulose composite sponges exhibited higher MVTR than the cellulose sponges without chitosan. The sponges as medical dressing with higher MVTR showed faster drying of the wound and tendency to produce eschars, whereas the ones with lower MVTR would cause the accumulation of exudate and open up the risk of bacterial growth. The presence of chitosan particles made the cellulose sponge more suitable as a potential candidate for wound dressing applications.

Swelling characteristics

The swelling ability of the cellulose sponge plays an important role in evaluating its property used as medical dressing. The swelling kinetics of the chitosan/cellulose composite sponge were evaluated in deionized water at 37 °C for 3 h. The effects of chitosan weight ratios on SRs were also analyzed and results are presented in Fig. 7. All the samples were characterized by a fast swelling directly after the immersion in deionized water. The water uptake ability of the cellulose sponge without chitosan particles was approximately 31 times of its weight in water, owing to the hydrophilic skeleton and the microporous network structure of cellulose. However,

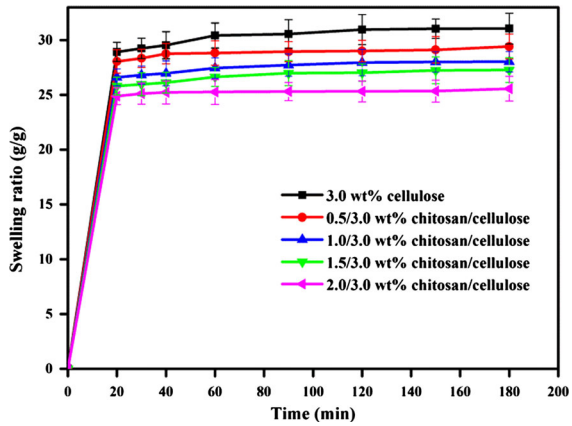

Fig. 7 Swelling kinetics of the chitosan/cellulose composite sponges with distinct chitosan content

with increasing chitosan percentage, the SR declined slightly. This might be attributed to the insolubility of chitosan in deionized water, due to the existence of $–NH_2$ groups, resulting in the shrinkage of the sponge network. Moreover, it is well known that the cross-linking density is one of the important factors for determining the water absorbency of sponges (Chang et al. 2010). The higher percentage of the chitosan, the more hydrogen bonds would be generated. As a result, the physical cross-linking density of the chitosan/cellulose composite sponges was increased by more intermolecular hydrogen bonds and chain entanglements. This would in turn form a more compact network structure, resulting in the decrease of SR.

Mechanical properties

The dependence of chitosan content on the breaking strength and elongation at break of the chitosan/cellulose composite sponges is plotted in Fig. 8. It was observed that the chitosan content had a profound effect on the mechanical property of the cellulose composite sponges. The breaking strength of the sponges increased from 0.09 to 0.32 MPa with increasing chitosan content from 0.0 to 1.0 wt%. The pure cellulose sponges displayed weak mechanical properties due to their inherent instability of the porous structure. The hydrogen bonding interaction between the hydroxyl groups of cellulose and chitosan favored a good interface between the matrix and the filler. This led to relatively higher breaking strengths of the chitosan/cellulose composite sponges. On the other hand, chitosan particles acted as connections

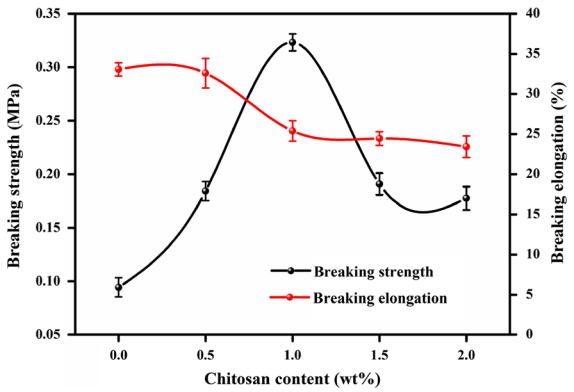

Fig. 8 Breaking strength and elongation of the chitosan/cellulose composite sponges with 3.0 wt% cellulose

between the pores to produce a linkage of the interconnecting pores and facilitate a uniform distribution. The well-dispersed chitosan particles also enhanced the overall mechanical performance of the composite structure. The high mechanical strength of the chitosan/cellulose composite sponges may result from efficient load transfer to the porous network, leading to a more uniform stress distribution and minimization of the stress concentration area (Khan et al. 2012).

Based on the above experimental finding, it was demonstrated that the optimum chitosan loading to get the best breaking strength value was at 1.0 wt%. With a higher concentration, the breaking strength tended to decrease. With the addition of chitosan particles higher than 1.0 wt%, the particles would aggregate together, acting as fracture weakness, which resulted in the drop of mechanical properties. Furthermore, the breaking elongation of the cellulose composite sponges decreased with increasing chitosan content. Filler-reinforced sponges usually tend to become more brittle as the concentration of the reinforcing particles increases (Rhim 2011). Such a decrease in breaking elongation indicated that the incorporation of chitosan particles into the cellulose matrix resulted in strong interactions between the filler and the matrix, which restricted the large deformation of the cellulose sponge. For the chitosan/cellulose composite sponges with 1.5 and 2.0 wt% chitosan particles, the decrease in both the breaking strength and elongation was due to the aggregation of the stiff chitosan particles. In sum, chitosan/cellulose composite sponges with improved mechanical properties and water absorption could be obtained by the addition of proper amount of chitosan particles.

Antibacterial activity

The antibacterial activities of chitosan/cellulose composite sponges with different chitosan contents were tested according to the inhibition zone method using *S. aureus* and *E. coli* bacteria. Bacterial growth underneath and around the sponges was observed in Fig. 9. The main criterion was the formation of the inhibition zone around the disk. Similar experiments were performed with chitosan-free cellulose sponges, in which no exclusion area was observed. It was evident that all the chitosan/cellulose composite sponges had good antibacterial activities against both bacteria as the obtained average inhibition zones were >2 mm. In addition, increasing chitosan concentration from 1.0 to 2.0 wt% did not significantly improve the exclusion area.

The cellulose composite sponges as medical dressing must constitute a barrier against external contaminating microorganisms and exhibit broad-spectrum antimicrobial activities to control the colonization of microorganisms in the wounded area. Thus, 1.0 wt% chitosan particles was a good candidate, which was sufficiently effective for both bacteria due to the average inhibition zones being greater than 6 mm. In the case of *S. aureus*, the exclusion area surrounding the composite sponges was thinner than that for *E. coli*. This indicated that *S. aureus* was probably less sensitive to chitosan particles than *E. coli*.

Table 2 clearly demonstrated the antibacterial activities of the chitosan/cellulose composite sponges with the activity increasing as a function of chitosan concentration. As compared to *S. aureus*, the chitosan/cellulose composite sponges exhibited slightly higher inhibition rate against *E. coli*. The inhibition rates against both bacteria were not changed significantly with the increase of chitosan content from 1.0 to 2.0 wt%.

The chitosan/cellulose composite sponges showed remarkably good antibacterial abilities to both bacteria by two possible mechanisms (Raafa et al. 2008). On the one hand, the chitosan particles can be absorbed onto the bacteria cell wall by the interaction between the positive charges of amino group in chitosan molecules and the negative charges on the bacteria cell wall. Then a layer of polymeric membrane was

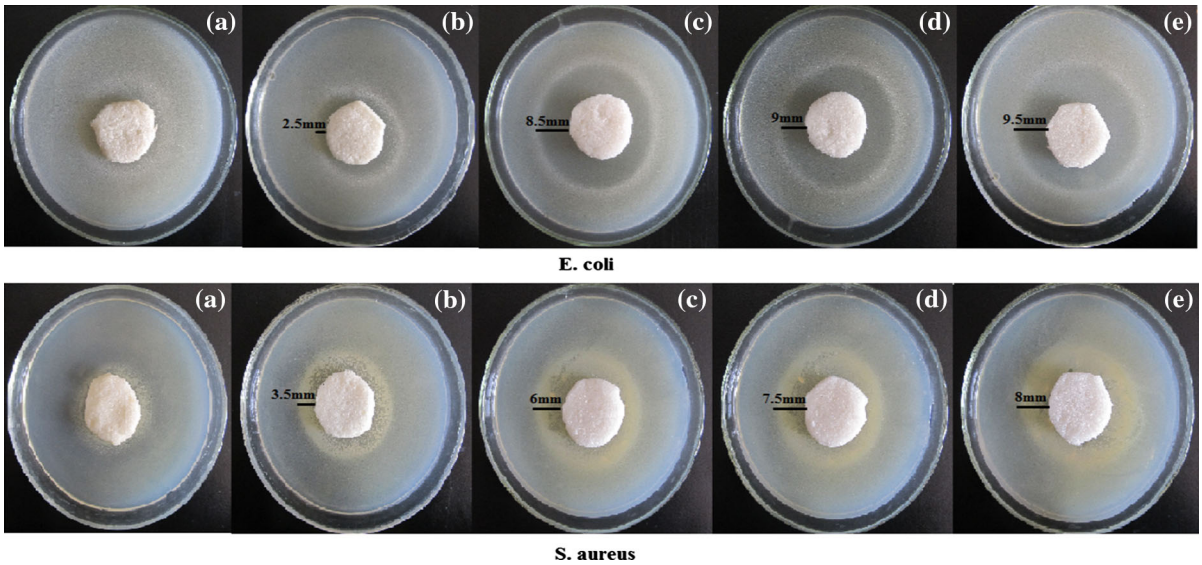

Fig. 9 Antimicrobial activities of the chitosan/cellulose composite sponges with different chitosan concentration against *S. aureus* and *E. coli*: (**a**) 0.0 wt%, (**b**) 0.5 wt%, (**c**) 1.0 wt%, (**d**) 1.5 wt% and (**e**) 2.0 wt%

Table 2 Antibacterial activities of the chitosan/cellulose composite sponges against *S. aureus* and *E. coli*

Sample	*S. aureus*			*E. coli*		
	CFU ($\times 10^4$ ml)		Inhibitory rate (%)	CFU ($\times 10^4$ ml)		Inhibitory rate (%)
Blank	3.80	4.00	–	4.40	5.30	–
Positive control[a]	4.10	0.45	89.02	4.10	0.58	85.85
0.5 wt%	4.00	0.77	80.75	4.20	0.72	82.81
1.0 wt%	4.20	0.18	95.68	4.30	0.05	98.89
1.5 wt%	4.10	0.12	97.03	4.50	0.04	99.15
2.0 wt%	4.00	0.06	98.33	4.30	0.01	99.69

[a] The commercial antibacterial agent-treated substrate as positive control with the concentration of 0.5 wt%

formed on the surface of the cell membrane. This polymeric membrane changed the perm-selectivity of the cell membrane and prevented the assimilation of nutrient substances, resulting in the loss of the cytoplasm and the separation of the cell wall. Typical bacterial cell destruction was due to the interaction with an amino functionalized surface. On the other hand, chitosan particles absorbed the cytoplasm with negative charges by penetrating into the cells. Then the flocculation occurred and harassed the normal physiological activities of the cells. In this way chitosan particles inhibited the growth of the bacteria and killed some of them.

Conclusions

The chitosan/cellulose biocomposite sponge was successfully prepared with [AMIM]Cl ionic liquid by a vacuum freeze drying process. The chitosan particles as reinforcement in the cellulose composite sponges distributed in a size range of 0.8–1.5 μm with a poly dispersity index of 0.326. The chitosan/cellulose composite sponge displayed a more uniform pore size distribution and dimensional regularity than that without chitosan. FTIR showed that no other chemical reaction occurred besides breakage of hydrogen bonds during the dissolution and regeneration processes of

cellulose. The absorption peak shift from 3,340 to 3,400 cm^{-1} indicated that hydrogen bonds were formed between hydroxyl groups of cellulose and chitosan. Although the SR slightly decreased with the increase of chitosan content, the porosity of the sponges increased from 60.1 to 75.94 % and the MVTR at 24 h increased to 90.2 g/(m^2h), which would be adequate for wound dressing. In addition, increasing chitosan content from 0.0 to 1.0 wt% enhanced the breaking strength of the sponges from 0.09 to 0.32 MPa. The chitosan/cellulose composite sponge exhibited excellent antibacterial activity against *S. aureus* and *E. coli*. The incorporation of chitosan particles by this method presented here improved the overall performance of the cellulose sponge as a potential candidate for wound dressing applications.

Acknowledgments The authors wish to thank National Natural Science Foundation of China (21174055),Graduate Students Innovation Project of Jiangsu Province in China (CXZZ1207246) and the Fundamental Research Funds for the Central Universities (JUDCF10038).

References

Archana D, Dutta J, Dutta PK (2013a) Evaluation of chitosan nano dressing for wound healing: characterization, in vitro and in vivo studies. Int J Biol Macromol 57:193–203

Archana D, Singh BK, Dutta J, Dutta PK (2013b) In vivo evaluation of chitosan–PVP–titanium dioxide nanocomposite as wound dressing material. Carbohydr Polym 95:530–539

Archana D, Upadhyay L, Tewari RP, Dutta J, Huang YB, Dutta PK (2013c) Chitosan–pectin–alginate as a novel scaffold for tissue engineering applications. Indian J Biotechnol 12:475–482

Cao Y, Wu J, Zhang J, Li H, Zhang Y, He J (2009) Room temperature ionic liquids (RTILs): a new and versatile platform for cellulose processing and derivatization. Chem Eng J 147:13–21

Chang C, Zhang L (2011) Cellulose-based hydrogels: present status and application prospects. Carbohydr Polym 84:40–53

Chang C, Zhang L, Zhou J, Zhang L, Kennedy JF (2010) Structure and properties of hydrogels prepared from cellulose in NaOH/urea aqueous solutions. Carbohydr Polym 82:122–127

Cui W, Kim DH, Imamura M, Hyon SH, Inoue K (2001) Tissue-engineered pancreatic islets: culturing rat islets in the chitosan sponge. Cell Transplant 10:499–502

Deng M, Zhou Q, Du A, Kasteren J, Wang Y (2009) Preparation of nanoporous cellulose foams from cellulose–ionic liquid solutions. Mater Lett 63:1851–1854

Feng L, Chen Z (2008) Research progress on dissolution and functional modification of cellulose in ionic liquids. J Mol Liq 142:1–5

Heinze T, Dorn S, Schöbitz M, Liebert T, Köhler S, Meister F (2008) Interactions of ionic liquids with polysaccharide-2: cellulose. Macromol Symp 262:8–22

Jayakumar R, Menon D, Manzoor K, Nair SV, Tamura H (2010) Biomedical applications of chitin and chitosan based nanomaterials-A short review. Carbohydr Polym 82:227–232

Jayakumar R, Prabaharan M, Kumar PTS, Nair SV, Tamura H (2011) Biomaterials based on chitin and chitosan in wound dressing applications. Biotechnol Adv 29:322–337

Jin H, Zha C, Gu L (2007) Direct dissolution of cellulose in NaOH/thiourea/urea aqueous solution. Carbohydr Res 342:851–858

Jin AX et al (2009) Comparative characterization of degraded and non-degradative hemicelluloses from barley straw and maize stems: composition, structure, and thermal properties. Carbohydr Polym 78:609–619

Khan A et al (2012) Mechanical and barrier properties of nanocrystalline cellulose reinforced chitosan based nanocomposite films. Carbohydr Polym 90:1601–1608

Kofuji K, Ito T, Murata Y, Kawashima S (2001) Biodegradation and drug release of chitosan gel beads in subcutaneous air pouches of mice. Biol Pharm Bull 24:205–208

Kondo T, Kasai W, Brown RM (2004) Formation of nematic ordered cellulose and chitin. Cellulose 11:463–474

Lai HL, Abu'Khalil A, Craig DQM (2003) The preparation and characterisation of drug-loaded alginate and chitosan sponges. Int J Pharm 251:175–181

Lee YM et al (2000) Tissue engineered bone formation using chitosan/tricalcium phosphate sponges. J Periodontol 71:410–417

Li Q, Zhou JP, Zhang LN (2009) Structure and properties of the nanocomposite films of chitosan reinforced with cellulose whiskers. J Polym Sci Pol Phys 47:1069–1077

Liang S, Zhang L, Xu J (2007) Morphology and permeability of cellulose/chitin blend membranes. J Membrane Sci 287:19–28

Luo K, Yin J, Khutoryanskaya OV, Khutoryanskiy VV (2008) Mucoadhesive and elastic films based on blends of chitosan and hydroxyethylcellulose. Macromol Biosci 8:184–192

Mi FL et al (2001) Fabrication and characterization of a sponge-like asymmetric chitosan membrane as a wound dressing. Biomaterials 22:163–173

Mi FL et al (2002) Control of wound infections using a bilayer chitosan wound dressing with sustainable antibiotic delivery. J Biomed Mater Res A 59:438–449

Mohamed NA, EI-Ghany NAA (2012) Synthesis and antimicrobial activity of some novel tereohthaloyl thiourea cross-linked carboxymethyl chitosan hydrogels. Cellulose 19:1879–1891

Morgado DL, Frollini E, Castellan A, Rosa DS, Coma V (2011) Biobased films prepared from NaOH/thiourea aqueous solution of chitosan and liner cellulose. Cellulose 18:699–712

Muzzarelli RAA (2009) Chitins and chitosans for the repair of wounded skin, nerve, cartilage and bone. Carbohydr Polym 76:167–182

Nair LS, Laurencin CT (2007) Biodegradable polymers as biomaterials. Prog Polym Sci 32:762–798

Novotna K, Havelka P, Sopuch T et al (2013) Cellulose-based materials as scaffolds for tissue engineering. Cellulose 20:2263–2278

Park YL et al (2000) Platelet derived growth factor releasing chitosan sponge for periodontal bone regeneration. Biomaterials 21:153–159

Pei Y, Wang XY, Huang WH, Liu P, Zhang LN (2013) Cellulose-based hydrogels with excellent microstructural replication ability and cytocompatibility for microfluidic devices. Cellulose 20:1897–1900

Pulkkinen H, Tiitu V, Lammentausta E, Hämäläinen ER, Kiviranta I, Lammi MJ (2006) Cellulose sponge as a scaffold for cartilage tissue engineering. Bio-Med Mater Eng 16:S29–S35

Raafa D, Bargen KV, Haas A, Sahl HG (2008) Insights into the mode of action of chitosan as an antibacterial compound. Appl Environ Microb 74:3764–3773

Raymond S, Kvick A, Chanzy H (1995) The structure of celluloseII: A revisit. Macromolecules 28:8422–8425

Rhim JW (2011) Effect of clay contents on the mechanical and water vapor barrier properties of agar-based nanocomposite films. Carbohydr Polym 86:691–699

Rogers RD, Seddon KR (2003) Ionic liquids-solvents of the future? Science 302:792–793

Shieh JJ, Huang RYM (1998) Chitosan/N-methylol nylon 6 blend membranes for the prevaporation separation of ethanol-water mixtures. J Membrane Sci 148:243–255

Singla AK, Chawla M (2001) Chitosan: some pharmaceutical and biological aspects—an update. J Pharm Pharmacol 53:1047–1067

Stefanescu C, Daly WH, Negulescu II (2012) Bicomposite films prepared from ionic liquid solutions of chitosan and cellulose. Carbohydr Polym 87:435–443

Swatlosti RP, Spear SK, Holbrey JD, Rogers RD (2002) Dissolution of cellulose with ionic liquids. J Am Chem Soc 124:4974–4975

Takegawa A, Murakami M, Kaneko Y, Kadokawa J (2010) Preparation of chitin/cellulose composite gels and films with ionic liquids. Carbohydr Polym 79:85–90

Tsioptsias C, Stefopoulos A, Kokkinomalis I, Papadopoulou I, Panayiotou C (2008) Development of micro- and nanoporous composite materials by processing cellulose with ionic liquids and supercritical CO_2. Green Chem 10:965–971

Wu Y et al (2004) Preparation and characterization on mechanical and antibacterial properties of chitosan/cellulose blends. Carbohydr Polym 57:435–440

Zhang L, Guo J, Du Y (2002) Morphology and properties of cellulose/chitin blends membranes from NaOH/thiourea aqueous solution. J Appl Polym Sci 86:2025–2032

Zhang S, Li F, Yu J, Hsieh YL (2010) Dissolution behavior and solubility of cellulose in NaOH complex solution. Carbohydr Polym 81:668–674